care and the offspring traits it influences in ways not predicted by traditional genetic models (*9*, *19*, *28*).

Much theoretical work has focused on the importance of honest signaling in social interactions (*2*, *4*, *6*, *29*). How do we interpret our results that signaling is affected by both condition and genotype in the context of honest signaling models? There are two possibilities. First, signal variation completely reflects differences in condition, but an individual's condition is influenced by both environmental and genetic factors. Even when all individuals experience similar environments, individuals will vary in condition because some individuals have better genotypes than others. Therefore, the genes that influence condition also affect signaling. The second possibility is that all genotypes signal more strongly with decreasing condition, but the absolute strength of signal produced for a given condition level varies among genotypes. In this case, signaling is only partially honest because it only partially reflects condition.

**References and Notes**


1. R. L. Trivers, *Am. Zool.* **14**, 249 (1974).
2. H. C. J. Godfray, *Nature* **376**, 133 (1995).
3. D. W. Mock, G. A. Parker, *The Evolution of Sibling Rivalry* (Oxford Univ. Press, New York, 1997).
4. A. Grafen, *J. Theor. Biol.* **144**, 517 (1990).
5. H. C. J. Godfray, *Nature* **352**, 328 (1991).
6. R. A. Johnstone, *Proc. Natl. Acad. Sci. U.S.A.* **96**, 12644 (1999).
7. C. T. Bergstrom, M. Lachmann, *Proc. Natl. Acad. Sci. U.S.A.* **95**, 5100 (1998).
8. M. Kölliker, M. W. G. Brinkhof, P. Heeb, P. S. Fitze, H. Richner, *Proc. R. Soc. London B* **267**, 2127 (2000).
9. J. M. Cheverud, A. J. Moore, in *Quantitative Genetic Studies of Behavioral Evolution*, C. R. B. Boake, Ed. (Univ. of Chicago Press, Chicago, 1994), pp. 67–100.
10. M. J. Wade, in *Maternal Effects as Adaptations*, T. Mousseau, C. Fox, Eds. (Oxford Univ. Press, New York, 1999), pp. 5–21.
11. J. B. Wolf, *Evolution* **54**, 1882 (2000).
12. _____, E. D. Brodie III, *Evolution* **52**, 299 (1998).
13. Female burrower bugs, *S. cinctus*, were collected from fields of *Lamium purpureum* in Bloomington, IN, in April 2000. Subjects were housed individually in 100 mm by 15 mm petri dishes with sand substrate and a plastic shelter until clutches were laid.
14. R. W. Sites, J. E. McPherson, *Ann. Entomol. Soc. Am.* **75**, 210 (1982).
15. S. L. Kight, *Anim. Behav.* **53**, 105 (1997).
16. _____, *Physiol. Entomol.* **23**, 38 (1998).
17. A. F. Agrawal, E. D Brodie III, J. Brown, unpublished data.
18. D. W. Tallamy, W. P. Brown, *Anim. Behav.* **57**, 727 (1999).
19. M. Kirkpatrick and R. Lande, *Evolution* **43**, 485 (1989).
20. Experiment I: Cross-fostering was achieved by placing each mother overnight in a small petri dish (60 mm by 15 mm) with an unrelated clutch 5 days after egg deposition. Under these conditions, adoption rate was high (>90%). Clutches and foster mothers were transferred into large petri dishes (150 mm by 15 mm) containing a plastic shelter. The number of offspring from each clutch was recorded upon hatching (~10 days after laying). Three bottle caps were distributed in the petri dish, and each cap was filled with 12 *L. purpureum* nutlets. The number of nutlets remaining in each dish was scored daily, and the total number of nutlets removed was recorded as a measure of provisioning. Each dish was restocked with 12 nutlets daily until the offspring reached third stadium. Mothers were frequently observed transporting nutlets from food dishes to the shelter, but offspring were never observed moving nutlets. Large numbers of nutlets were found in and around the shelter where offspring were usually clustered. Because burrower bugs have sucking mouthparts, adults do not need to remove nutlets from the food dish in order to consume their contents. Nutlets were rarely found in other areas of the experimental arena.
21. Experiment II: Immediately after hatching, 18 clutches were counted, split in half, and placed with an unrelated foster mother. Only clutches of sufficient size to generate half-clutches within the natural range of variation of full clutch size were used. Clutches and foster mothers were moved into experimental arenas as described above. For each pair of related half-clutches, one half-clutch was assigned to the "no-nutlet removal" (control) treatment and the other to the "nutlet removal" treatment. In each treatment, the nutlets remaining in each dish were counted and dishes were restocked daily every 2 hours from 7:00 a.m. to 9:00 p.m. until the offspring reached the third stadium. In the nutlet removal treatment, all nutlets provisioned to offspring were removed every 2 hours during counting. All nutlets provisioned were left with offspring in the control treatment. In the no-nutlet treatment, offspring had limited opportunity to feed on provisioned nutlets before they were removed.
22. M. Lynch, B. Walsh, *Genetics and Analysis of Quantitative Traits* (Sinauer, Sunderland, MA, 1998).
23. As a control for the cross-fostering, some individuals were "mock-fostered." In this treatment, mothers and egg clutches experienced the same type of manipulation as with cross-fostering, except that mothers re-adopted their own (i.e., related) egg clutch rather than an unrelated egg clutch. No differences existed in the total number of nutlets provisioned to 46 mock-fostered and 153 cross-fostered clutches ($t$ = 0.892, df = 197). Neither did cross-fostering influence the size of offspring ($F_{1,193}$ = 2.15).
24. C. M. Rauter, A. J. Moore, *Proc. R. Soc. London B* **266**, 1691 (1999).
25. The influence of biological clutch size and foster clutch size on total nutlets provisioned was compared with the use of a multiple linear regression. We tested for effects of female body size (measured as pronotum width) in the same regression model, but no relation was apparent ($t$ = 0.69, df = 127). Therefore, we report the results of the regression of total nutlets provisioned on biological clutch size and foster clutch size only.
26. We tested this one-tailed hypothesis using a product-moment correlation between the number of nutlets provisioned per individual offspring to a family in the two treatments. For statistical analyses, we used the residual from the regression of total nutlets provisioned on clutch size as a measure of nutlets per individual offspring. The results remain qualitatively similar if the analysis is performed with either the total nutlets provided or the ratio of nutlets/individual offspring.
27. The association between the number of nutlets a mother provisioned to her unrelated foster clutch and the number of nutlets elicited by her biological clutch from an unrelated foster mother was assayed with product-moment correlation. Differences in clutch size among families were adjusted for using residuals from the regression of total provisioning on foster clutch size.
28. A. J. Moore, E. D. Brodie III, J. B. Wolf, *Evolution* **51**, 1352 (1997).
29. R. Kilner, R. A. Johnstone, *Trends Ecol. Evol.* **12**, 11 (1997).


30. We thank K. Quinlan for assistance with bug collection and husbandry. M. Maple and M. Wade provided helpful comments on the manuscript. This work was supported by NSF grant IBN-9896116 to E.D.B. III and a Natural Sciences and Engineering Research Council of Canada Fellowship to A.F.A.

15 February 2001; accepted 24 April 2001


# Sorting of Mannose 6-Phosphate Receptors Mediated by the GGAs


**Rosa Puertollano,[1]* Rubén C. Aguilar,[1]* Inna Gorshkova,[2] Robert J. Crouch,[2] Juan S. Bonifacino[1]†**



**The delivery of soluble hydrolases to lysosomes is mediated by the cation-independent and cation-dependent mannose 6-phosphate receptors. The cytosolic tails of both receptors contain acidic-cluster-dileucine signals that direct sorting from the trans-Golgi network to the endosomal-lysosomal system. We found that these signals bind to the VHS domain of the Golgi-localized, γ-ear–containing, ARF-binding proteins (GGAs). The receptors and the GGAs left the trans-Golgi network on the same tubulo-vesicular carriers. A dominant-negative GGA mutant blocked exit of the receptors from the trans-Golgi network. Thus, the GGAs appear to mediate sorting of the mannose 6-phosphate receptors at the trans-Golgi network.**


Lysosomal hydrolases are posttranslationally modified in the Golgi complex by the addition of mannose 6-phosphate groups that function as signals for sorting to lysosomes (*1*). The mannose 6-phosphate groups are recognized in the trans-Golgi network (TGN) by a cation-independent mannose 6-phosphate receptor (CI-MPR) or a cation-dependent mannose 6-phosphate receptor (CD-MPR). Both mannose 6-phosphate receptors (MPRs) mediate recruitment of the lysosomal hydrolases to clathrin-coated areas of the TGN, from which carrier vesicles deliver the MPR-hydrolase complexes to endosomes. The acidic pH of endosomes induces release


[1]Cell Biology and Metabolism Branch, National Institute of Child Health and Human Development, National Institutes of Health, Bethesda, MD 20892, USA. [2]Laboratory of Molecular Genetics, National Institute of Child Health and Human Development, National Institutes of Health, Bethesda, MD 20892, USA.

*These authors contributed equally to this work.
†To whom correspondence should be addressed. E-mail: juan@helix.nih.gov

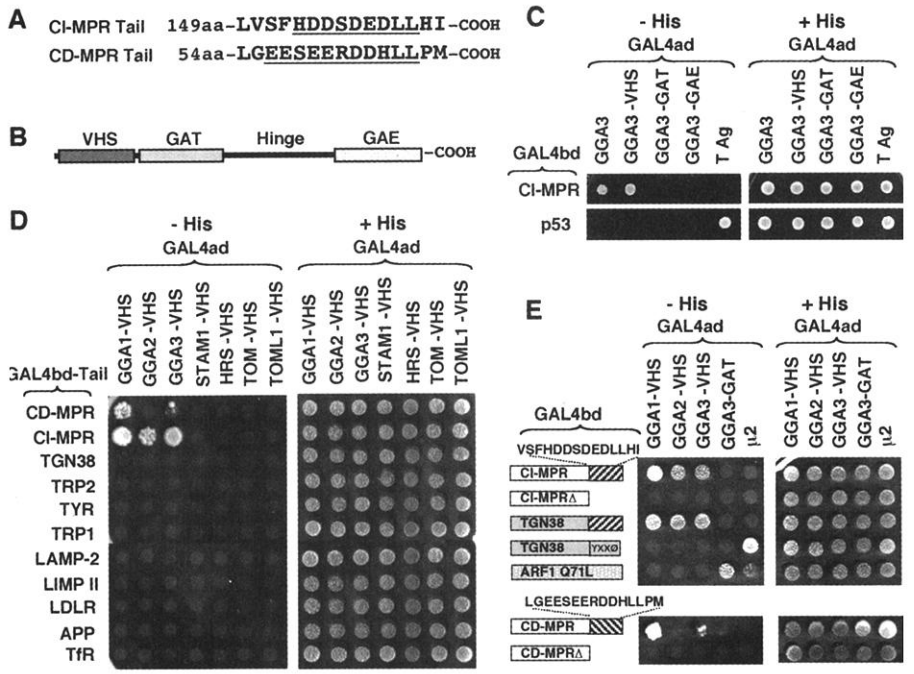


**Fig. 1.** Analysis of interactions between MPR cytosolic tail sequences and the GGAs with the yeast two-hybrid system. (**A**) COOH-terminal sequences of the CI-MPR and CD-MPR cytosolic tails. Acidic-cluster-dileucine signals are underlined. (**B**) Domain organization of the GGAs. (**C** to **G**). Yeast cells were cotransformed with plasmids encoding GAL4bd fused to the cytosolic tail sequences or control proteins indicated on the left with GAL4ad fused to the proteins or protein domains indicated above each panel. The MPR constructs contained the terminal 113 of the 154–amino acid cytosolic tail of the CI-MPR and the terminal 41 of the 69–amino acid CD-MPR tail. Mouse p53, SV40 large T antigen (T Ag), μ2, and ARF1 Q71L were used as controls. Mutated residues are underlined. Cotransformed cells were spotted onto histidine-deficient (−His) or histidine-containing (+His) plates and incubated at 30°C as described (*14*). Growth on −His plates is indicative of interactions. TYR: tyrosinase; LDLR: LDL receptor; APP: β-amyloid precursor; TfR: transferrin receptor (*19*).

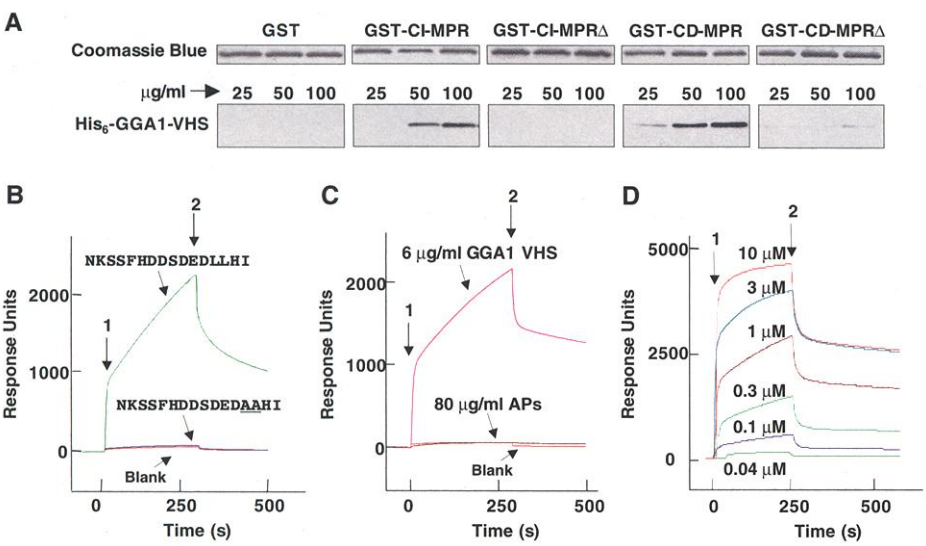


**Fig. 2.** Interactions of MPR signal sequences with the VHS domain of GGA1 in vitro. (**A**) Recombinant $His_6$-GGA1-VHS (25, 50, and 100 μg/ml) was tested for interactions with GST or GST fusion proteins bearing the tails of the CI-MPR or CD-MPR, or these tails with deletion of the acidic-cluster-dileucine signals shown in Fig. 1A (GST-CI-MPRΔ constructs). The GST fusion proteins were visualized by Coomassie blue staining, and bound $His_6$-GGA1-VHS was detected by immunoblotting with antibody to $His_6$ (*20*). (**B**) $His_6$-GGA1-VHS (6 μg/ml, ~0.3 μM) was injected (arrow 1) onto streptavidin-coated sensor chips loaded with N-biotinylated NKSSFHDDSDEDLLHI or NKSSFHDDSDEDAAHI peptides derived from the CI-MPR tail or with no peptide (blank). Dissociation of the protein was induced by injection of buffer containing 20 μM biotinylated NKSSFHDDSDEDLLHI to prevent rebinding (arrow 2). Flow rate: 20 μl/min. (**C**) $His_6$-GGA1-VHS (6 μg/ml) or a ~1:7 mixture of AP-1 and AP-2 (80 μg/ml) purified by gel filtration from extracts of bovine brain clathrin-coated vesicles (APs) were injected onto streptavidin-coated sensor chips loaded with N-biotinylated NKSSFHDDSDEDLLHI peptide. The blank corresponded to $His_6$-GGA1-VHS injected onto sensor chips without peptide. Flow rate: 20 μl/min. (**D**) Various concentrations of $His_6$-GGA1-VHS as indicated were injected onto streptavidin-coated sensor chips loaded with biotinylated NKSSFHDDSDEDLLHI peptide. The apparent equilibrium dissociation constant was calculated by nonlinear least-squares fitting of the data, assuming a single-site interaction model. Flow rate: 2 μl/min (*21*).

of the hydrolases from the MPRs, after which the hydrolases are transported to lysosomes while the MPRs return to the TGN for additional rounds of sorting.

Sorting of both MPRs from the TGN to endosomes is mediated by signals present in the cytosolic tails of the receptors (Fig. 1A). These signals consist of a cluster of acidic amino acid residues followed by two leucine residues (*2*, *3*). Early studies suggested that sorting of MPRs at the TGN was mediated by the clathrin-associated adaptor protein (AP) complex, AP-1 (*4*, *5*). However, AP-1 does not appear to bind the acidic-cluster-dileucine signals from the MPRs (*6*, *7*). In addition, a recent study has shown that disruption of AP-1 impairs retrograde transport of the MPRs from endosomes to the TGN (*8*). Thus, clathrin-associated proteins other than AP-1 might be responsible for the signal-mediated sorting of MPRs at the TGN. Prime candidates for this role are the Golgi-localized, γ -ear–containing, ARF-binding proteins (GGAs) (*9*–*12*). Three GGAs have been identified in humans (GGA1, GGA2, and GGA3) and two in yeast (Gga1p and Gga2p). These proteins are monomeric and display a modular structure consisting of a VHS (VPS27, Hrs, and STAM) domain of unknown function, a GAT domain that interacts with the guanosine 5′-triphosphate–bound form of ADP-ribosylation factors (ARF) (*9*, *10*, *13*), a hinge domain that interacts with clathrin (*13*), and a GAE domain that interacts with γ-synergin and other potential regulators of coat assembly (*11*) (Fig. 1B). Disruption of the two yeast genes encoding GGAs results in impaired sorting of procarboxypeptidase Y to the vacuole, the equivalent of the mammalian lysosome (*10*, *11*). These characteristics of the GGAs prompted us to test whether they could bind the cytosolic tails of the MPRs.

Analyses with the yeast two-hybrid system showed that the cytosolic tail of the human CI-MPR interacted with full-length GGA3 as well as with the ~150–amino acid VHS domain, but not the GAT or GAE domains of GGA3 (Fig. 1C). Further analyses revealed that the CI-MPR tail interacted with the VHS domains of all three GGAs and that the CD-MPR tail interacted with the VHS domains of GGA1 and, more weakly, GGA3 (Fig. 1D). These interactions were highly specific, because neither MPR tail bound to the VHS domains of STAM1, HRS, TOM1, and TOM1L1 (Fig. 1D). Likewise, we did not detect interactions between the GGA VHS domains and the cytosolic tails of TGN38, TRP2, tyrosinase, TRP1, LAMP-2, LIMP II, low density lipoprotein (LDL) receptor, β-amyloid precursor, and transferrin receptor (Fig. 1D), which contain either tyrosine-based sorting signals or dileucine-based sorting signals devoid of acidic clusters.

Deletion of the acidic-cluster-dileucine signals from the CI-MPR and CD-MPR tails abolished interactions with GGA VHS domains (Fig. 1E). Conversely, placement of the acidic-cluster-dileucine signal of the CI-MPR at the end of a 23–amino acid segment of the TGN38 cytosolic tail (*14*) conferred binding to the GGA VHS domains (Fig. 1E). The acidic-cluster-dileucine signal was thus both necessary and sufficient for interaction with the GGA VHS domains. Mutational analyses of the signals showed that the two leucines, as well as some of the acidic residues, were required for interactions (Fig. 1, F and G).

To corroborate the results of the yeast two-hybrid assays, we performed in vitro binding experiments. Glutathione-S-transferase (GST) pull-down assays showed specific binding of the recombinant VHS domain of GGA1 to the cytosolic tails of both MPRs (Fig. 2A). These interactions were abolished by deletion of the signals (Fig. 2A). Analysis by surface plasmon resonance spectroscopy confirmed the interaction of the recombinant GGA1 VHS domain with a biotinylated peptide comprising the acidic-cluster-dileucine

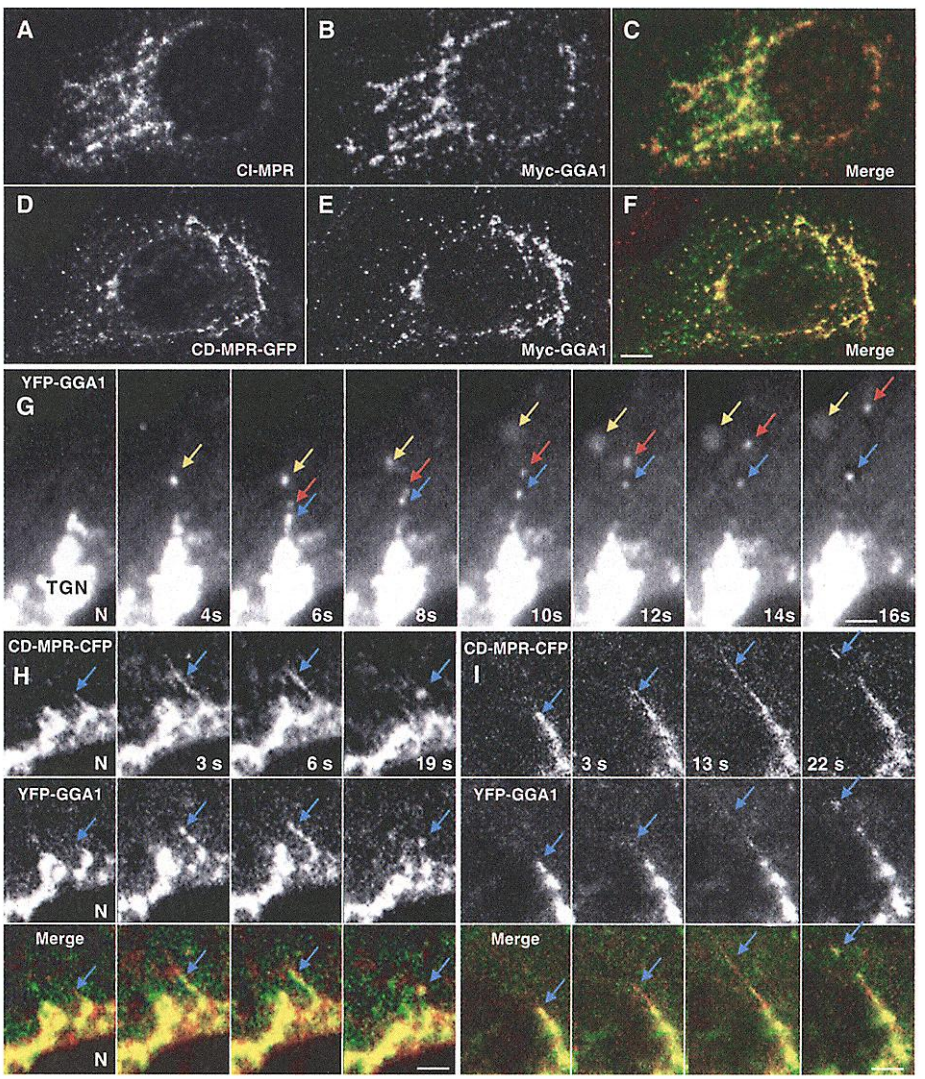


**Fig. 3.** Immunofluorescence microscopy analysis of GGA1 and MPR localization. (**A** to **C**) MDCK cells stably expressing MYC-GGA1 were stained with mouse monoclonal antibody (mAb) to the CI-MPR (MA1-066; Affinity BioReagents, Golden, CO) (A) and rabbit polyclonal antibody to the MYC epitope (BabCo, Richmond, CA) (B) followed by Alexa 488 anti-mouse immunoglobulin G (IgG) and Cy3 anti-rabbit IgG. (**D** to **F**) MDCK cells stably expressing MYC-GGA1 were transiently transfected with a construct encoding CD-MPR-GFP (D) and stained with mouse mAb to the MYC epitope (9E10; BabCo, Berkeley, CA) (E) and Cy3 anti-mouse IgG (*22*). (**G**) Time-lapse microscopy imaging sequence of live MDCK cells expressing YFP-GGA1. Images were acquired on a TILL Photonics microscope at the intervals indicated. Arrows track individual vesicles budding from the TGN. N: nucleus. For more details, see video 1 (*15*). (**H** and **I**) Confocal microscope imaging sequences of live MDCK cells coexpressing YFP-GGA1 and CD-MPR-CFP. Images were acquired at the intervals indicated. Arrows point to tubulo-vesicular structures containing both fluorescently labeled proteins. Bars: (A to F) 5 μm; (G to I), 1 μm. Transiently transfected cells grown in chambers were imaged as described (*13*).

signal of the CI-MPR (Fig. 2B). This interaction was completely abrogated by substitution of the two leucines with alanines (Fig. 2B). In agreement with other studies (*6*, *7*), a mixture of AP-1 and AP-2 purified from bovine brain did not show appreciable binding to the acidic-cluster-dileucine signal (Fig. 2C). Binding of various concentrations of GGA1-VHS to the CI-MPR tail peptide (Fig. 2D) allowed an estimation of the equilibrium dissociation constant at ~1 μM.

Immunofluorescence microscopy analyses showed good colocalization of endogenous CI-MPR (Fig. 3, A to C), as well as CD-MPR tagged at the COOH-terminus with the green fluorescent protein (GFP) (Fig. 3, D to F), with stably expressed MYC-GGA1 at the TGN and peripheral vesicles of MDCK cells. Time-lapse, confocal imaging of live MDCK cells expressing GGA1 tagged with the yellow fluorescent protein (YFP) revealed budding of tubulo-vesicular structures containing GGA1 from the TGN [Fig. 3G and video 1 (*15*)]. After detaching from the TGN, these structures migrated toward the peripheral cytoplasm at speeds of 1 to 4 μm/s [Fig. 3G and video 1 (*15*)]. Coexpressed CD-MPR tagged at the COOH-terminus with the cyan fluorescent protein (CFP) was present in the GGA1-containing tubulo-vesicular structures (Fig. 3, H and I), suggesting that these corresponded to intermediates that carry MPRs from the TGN.

Expression of moderate levels of a dominant-negative GGA1 VHS-GAT construct lacking the hinge and GAE domains caused accumulation of CD-MPR at the TGN and its depletion from the periphery (Fig. 4B, arrow), as previously observed for the CI-MPR (*13*). In contrast, this construct did not affect the localization of LAMP-1 to lysosomes (Fig. 4E), Tac (*14*) to the plasma membrane (Fig. 4H), and TGN38 to the TGN (Fig. 4K). At these moderate levels of GGA1 VHS-GAT expression, there was also no visible effect on the localization of AP-1 to the TGN and peripheral foci (Fig. 4N). Thus, GGA function was apparently required for CD-MPR exit from the TGN.

We have identified highly specific interactions of acidic-cluster-dileucine signals involved in sorting of MPRs at the TGN with the VHS domain of the GGAs. These interactions have the hallmarks of bona fide signal-recognition events, including (i) similar sequence requirements for interactions and for function of the signals in vivo (*2*, *3*); (ii) an affinity comparable to that of other well-characterized sorting signals for their recognition molecules (*14*, *16*, *17*); (iii) colocalization of the GGAs and the MPRs to the TGN and peripheral vesicles, and their exit from the TGN on the same tubulo-vesicular carriers; (iv) the properties of the GGAs as clathrin adaptors (*13*) and the requirement for clathrin for MPR sorting at the TGN (*18*); and (v) the ability of a dominant-negative GGA mutant to interfere with sorting of MPRs at the TGN. The elucidation of a specific signal-recognition function for the VHS domain completes the assignment of at least one function to each of the four GGA domains and establishes the GGAs as genuine sorting adaptors.

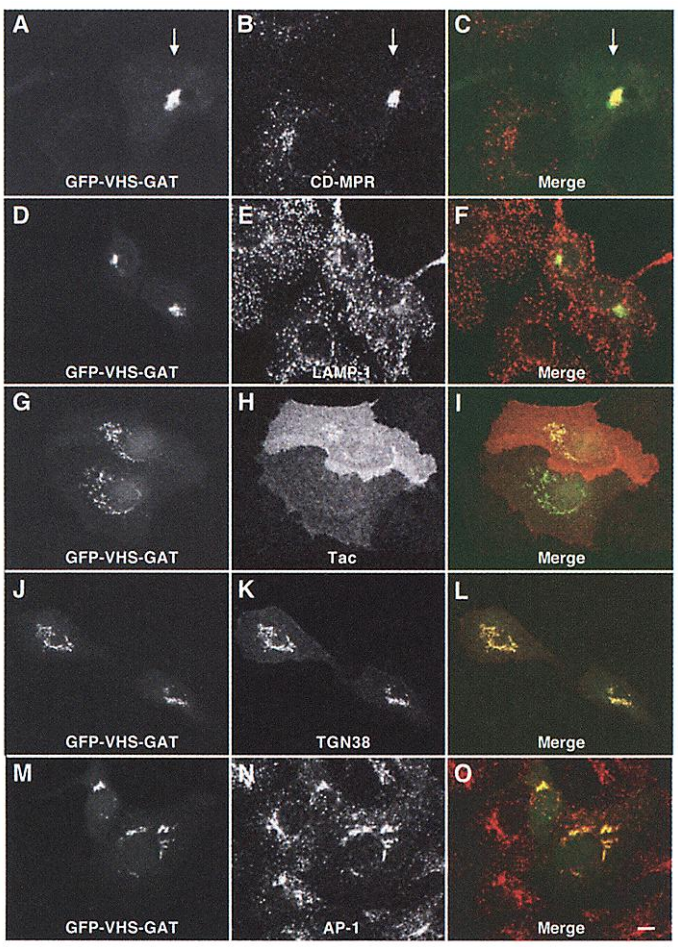


**Fig. 4.** Effect of GGA1 VHS-GAT expression on CD-MPR localization. COS-7 cells were transfected with plasmids encoding GFP-tagged GGA1 VHS-GAT (GFT-VHS-GAT) alone (**A** to **F**, **M** to **O**), GFP-VHS-GAT and Tac (**G** to **I**), or GFP-VHS-GAT and HA-TGN38 (**J** to **L**). Cells were immunostained with rabbit anti–CD-MPR (A to C), mouse anti–LAMP-1 (AC17) (D to F), rabbit anti-Tac (from our lab) (G to I), mouse anti-hemagglutinin epitope (BabCo) (J to L), or mouse anti–AP-1-γ (100/3, Sigma) (M to O) antibodies, followed by the corresponding Cy3 anti-rabbit or anti-mouse IgG. Bar: 15 μm.

### References and Notes


1. S. Kornfeld, *Annu. Rev. Biochem.* **61**, 307 (1992).
2. K. F. Johnson, S. Kornfeld, *J. Cell Biol.* **119**, 249 (1992).
3. H. J. Chen, J. Yuan, P. Lobel, *J. Biol. Chem.* **272**, 7003 (1997).
4. J. N. Glickman, E. Conibear, B. M. Pearse, *EMBO J.* **8**, 1041(1989).
5. F. Mauxion, R. Le Borgne, H. Munier-Lehmann, B. Hoflack, *J. Biol. Chem.* **271**, 2171 (1996).
6. S. Höning, M. Sosa, A. Hille-Rehfeld, K. von Figura, *J. Biol. Chem.* **272**, 1984 (1997).
7. Y. Zhu, B. Doray, A. Poussu, V.-P. Lehto, S. Kornfeld, *Science* **292**, 1716 (2001).
8. C. Meyer *et al.*, *EMBO J.* **19**, 2193 (2000).
9. A. L. Boman, C. J. Zhang, X. Zhu, R. A. Kahn, *Mol. Biol. Cell* **11**, 1241 (2000).
10. E. C. Dell'Angelica *et al.*, *J. Cell Biol.* **149**, 81 (2000).
11. J. Hirst *et al.*, *J. Cell Biol.* **149**, 67 (2000).
12. A. Poussu, O. Lohi, V. P. Lehto, *J. Biol. Chem.* **275**, 7176 (2000).
13. R. Puertollano, P. Randazzo, L. M. Hartnell, J. Presley, J. S. Bonifacino, *Cell* **105**, 93 (2001).
14. R. C. Aguilar *et al.*, *J. Biol. Chem.* **276**, 13145 (2001).
15. Supplementary data are available on *Science* Online at www.sciencemag.org/cgi/content/full/292/5522/1712/DC1.
16. W. Boll *et al.*, *EMBO J.* **15**, 5789 (1996).
17. R. Heilker, M. Spiess, P. Crottet, *Bioessays* **21**, 558 (1999).
18. S. H. Liu, M. S. Marks, F. M. Brodsky, *J. Cell Biol.* **140**, 1023 (1998).
19. Two-hybrid GAL4 DNA binding domain (GAL4bd) and GAL4 transcription activation domain (GAL4ad) fusion constructs were prepared by ligating cDNAs for different proteins or protein fragments into the pGBT9(TRP1) and pGAD424(LEU2) vectors, respectively (Clontech, Palo Alto, CA). Amino acid substitutions were made with the QuickChange mutagenesis kit (Stratagene, La Jolla, CA). Mating and transformation of these cells were done as described in the MATCHMAKER two-hybrid manual (Clontech). Recombinant constructs are described in the supplementary material (*15*).
20. GST or GST fusion proteins (0.1 mg/ml) were incubated with recombinant $His_6$-GGA1-VHS in 0.5 ml of 50 mM Hepes-KOH (pH 7.5), 150 mM KCl, 1 mM $MgCl_2$, 10% (v/v) glycerol, and 0.6 mg/ml bovine serum albumin for 2 hours at 4°C. Glutathione–Sepharose 4B (50 μl) was added and the incubation continued for an additional 30 min. The suspension was transferred to chromatography columns, washed extensively, and eluted in 20 mM glutathione. Samples were analyzed by SDS–polyacrylamide gel electrophoresis and immunoblotting with antibody to the $His_6$ tag (Clontech).
21. Surface plasmon resonance spectroscopy was performed at 25°C on a BIACORE 1000 instrument (*14*). The amount of biotinylated peptide captured on the chips was ~0.03 pmol/mm². Running buffer contained 50 mM Hepes-KOH (pH 7.5), 150 mM KCl, 1 mM $MgCl_2$, 1 mM EDTA, and 0.005% P20.

22. MDCK or COS-7 cells grown on cover slips were transfected with FuGENE-6 (Roche Molecular Biochemicals). At 15 to 20 hours after transfection, cells were fixed in methanol/acetone at −20°C for 10 min. Immunofluorescent staining and confocal microscopy were done as described (*10*).

23. We thank X. Zhu for technical assistance; J. Presley for help with fluorescence microscopy; L. Greene (APs), R. Lodge (CD-MPR-GFP), S. Kornfeld (rabbit anti–CD-MPR), and E. Rodríguez-Boulan (mouse anti–LAMP-1) for reagents; J. Lippincott-Schwartz, C. Jackson, C. Mullins. M. Boehm, and S. Caplan for comments on the manuscript; and S. Kornfeld for sharing unpublished observations. R.P. was supported by the Fundación Ramón Areces.

16 March 2001; accepted 27 April 2001

# Binding of GGA2 to the Lysosomal Enzyme Sorting Motif of the Mannose 6-Phosphate Receptor

**Yunxiang Zhu,[1] Balraj Doray,[1] Anssi Poussu,[2] Veli-Pekka Lehto,[2] Stuart Kornfeld[1]***

**The GGAs are a multidomain protein family implicated in protein trafficking between the Golgi and endosomes. Here, the VHS domain of GGA2 was shown to bind to the acidic cluster–dileucine motif in the cytoplasmic tail of the cation-independent mannose 6-phosphate receptor (CI-MPR). Receptors with mutations in this motif were defective in lysosomal enzyme sorting. The hinge domain of GGA2 bound clathrin, suggesting that GGA2 could be a link between cargo molecules and clathrin-coated vesicle assembly. Thus, GGA2 binding to the CI-MPR is important for lysosomal enzyme targeting.**

The CI-MPR serves a key role in the biogenesis of lysosomes (*1*). This receptor binds newly synthesized lysosomal enzymes through their mannose 6-phosphate recognition marker in the trans-Golgi network (TGN). The ligand-receptor complex is then packaged into transport vesicles that dock on endosomal compartments where the enzymes are released and subsequently transferred to lysosomes. Efficient lysosomal enzyme sorting by this intracellular pathway is dependent on an acidic cluster–dileucine motif near the COOH-terminus of the cytoplasmic tail of the receptor, as shown by the finding that mutations in this motif result in hypersecretion of the enzymes (*2–5*). In spite of the importance of this sorting signal, the binding partner of the acidic cluster–dileucine motif has not been identified.

The GGAs are a newly described protein family named for being Golgi-localized, γ-ear–containing, ARF-binding proteins (*6–10*). Each of the five members (two in yeast and three in mammalian cells) contains four domains. The COOH-terminal domain is homologous to the ear domain of the γ-adaptin subunit of AP-1. This domain is linked to the GAT domain by a hinge region. The GAT domain binds ARF–guanosine triphosphate and mediates membrane association with the TGN. The $NH_2$-terminal region contains a VHS domain to which no function has been assigned.

Deletion of the yeast GGA genes impairs sorting of carboxypeptidaseY from the Golgi to the vacuole and delivery of Pep12p from the Golgi to late endosomes (*7*, *8*, *11*, *12*), suggesting that the GGAs may be required for the assembly of transport vesicles (*12*). These molecules have been localized to coated buds in the TGN in mammalian cells but have not been detected in clathrin-coated vesicles (CCVs) (*7*, *8*), and no specific function for Golgi-associated GGAs has been defined.

We hypothesized that these proteins might interact with receptors such as the CI-MPR to facilitate their packaging into transport vesicles. To test whether GGA2 binds the CI-MPR, we solubilized rat liver Golgi membranes with detergent and used them as a source of receptor for binding to glutathione *S*-transferase (GST) or GST-GGA2 coupled to glutathione beads. The CI-MPR bound specifically to GST-GGA2 (Fig. 1A). By contrast, the polymeric immunoglobulin A receptor (Fig. 1A), Lamp1, Lamp2, LimpII, and TGN38 did not bind (*13*). Furthermore, purified full-length CI-MPR bound directly to GST-GGA2, whereas soluble CI-MPR lacking the cytoplasmic tail failed to bind (Fig. 1A). We next determined which domain of GGA2 mediates the interaction with the CI-MPR. GST-GGA2 COOH-end (residues 170 to 613) with the VHS domain deleted failed to bind the receptor, implicating the VHS domain in this interaction (Fig. 1A). However the GST-GGA2 VHS domain by itself (residues 29 to 165) also failed to bind the CI-MPR. Extension of the VHS domain by 23 amino acids into the GAT domain (from residues 165 to 188) restored receptor binding (Fig. 1B). Addition of more residues did not increase receptor binding.

To identify the determinant in the CI-MPR cytoplasmic tail that binds the VHS domain, we used a library of CI-MPR negative mouse L cell fibroblast lines that had been stably transfected with cDNAs encoding either wild-type bovine CI-MPR or mutants with various deletions or amino acid substitutions in the cytoplasmic tail (Fig. 1C) (*2*, *4*, *5*). Cell pellets were solubilized with detergent and tested for binding to GST-GGA2 in pull-down binding assays. Mutant bovine CI-MPRs with COOH-terminal deletions of 40 or more amino acids of the 163–amino acid cytoplasmic tail were greatly impaired in binding to GST-GGA2 (Fig. 1D). We next tested the AC series of mutants, each having four consecutive residues changed to alanines, starting at the COOH-terminal LLHI (*14*) sequence of the murine CI-MPR (*5*). Mutants AC1 to 3 were severely impaired in binding GST-GGA2 (<5% of wild type), whereas mutants AC4 and AC5 exhibited only a small decrease in binding (80% of wild type), and AC8 was somewhat more impaired (35% of wild type) (Fig. 1, E and F). Receptors with point mutations in this distal region (D157A, D158A, D160A, E161A, and D162A) (*14*) also exhibited poor binding to GST-GGA2 (12 to 20% of wild type) (Fig. 1G). The cytoplasmic tail of CI-MPR contains a second acidic motif that lacks the dileucine sequence (Fig. 1C). Mutations in this motif (AC17 and AC18) did not substantially affect GGA2 binding, indicating that this upstream motif is not necessary for GGA2 binding (Fig. 1F). Finally, a mutant receptor with the COOH-terminal LLHI sequence deleted (Δ4) failed to bind GST-GGA2 (Fig. 1F). These results demonstrate that the acidic cluster–dileucine sequence $^{157}$DDSDEDLLHI$^{166}$ (*14*) mediates the interaction with the VHS domain of GGA2 and establish a very strong correlation between reduced GGA2 binding and defective lysosomal enzyme sorting. The failure of rat LimpII with a DEXXXLL (*14*) motif in its cytoplasmic tail to bind GGA2 illustrates the specificity of this interaction.

The CI-MPR has been localized to AP-1–containing CCVs on the TGN (*15*). According-

[1]Department of Internal Medicine, Washington University School of Medicine, 660 South Euclid Avenue, St. Louis, MO 63110, USA. [2]Department of Pathology, University of Oulu, FIN-90410 Oulu, Finland.

*To whom correspondence should be addressed. E-mail: skornfel@im.wustl.edu